Journal of Thermal Analysis and Calorimetry, Vol. 93 (2008) 1, 87–93

THREE-PHASE CYANATE ESTER COMPOSITES WITH FUMED SILICA AND NEGATIVE-CTE REINFORCEMENTS

*W. K. Goertzen and M. R. Kessler**

Department of Materials Science and Engineering, Iowa State University, 2220 Hoover Hall, Ames, IA 50011, USA

Three-phase cyanate ester adhesives have been developed using a bisphenol E cyanate ester resin, fumed silica, and negative-CTE (coefficient of thermal expansion) reinforcements: short carbon fiber or zirconium tungstate (ZrW_2O_8). Fumed silica was used to impart thixotropic behavior on the resin and decrease settling in the adhesives. The cured composites were evaluated using various thermal analysis techniques for their thermal-mechanical properties.

Composites with short carbon fiber showed enhanced modulus and decreased thermal expansion (70% reduction for 20 vol%) and showed little phase separation. While settling of the dense ceramic particles could not be completely eliminated for the zirconium tungstate composites through rheological modification of the adhesive with added fumed silica, a reduction in CTE of 84% was achieved in the composite (58 vol%) compared to the neat resin. In addition, the effect of thermal history on the cure and temperature induced ZrW_2O_8 phase transitions, and their corresponding influence on thermal strains *vs.* temperature, are examined by thermomechanical analysis.

Keywords: *composites, negative thermal expansion, thermal expansion, thermomechanical analysis*

Introduction

Cyanate esters are a class of high-temperature thermosetting polymers, which have excellent thermal and mechanical properties. The bisphenol E cyanate ester (BECy) is a unique type of cyanate ester that is under investigation for use as the matrix material for adhesives with enhanced ambient temperature processability. BECy monomer has a low viscosity at room temperature and excellent storage characteristics and the cured polymer has a high glass transition temperature and excellent mechanical properties [1, 2].

Settling and phase separation can be a problem in cyanate ester adhesives because of the high density of fillers and the low density of the BECy monomer. This problem is also complicated because the already low viscosity of the BECy during storage is even lower during the initial stages of cure at elevated temperature before gelation has occurred. Fumed silica (FS) has been used in many systems to reduce phase separation and settling [3, 4]. This work covers initial investigations into three-phase composite materials that use fumed silica/cyanate ester nanocomposites, which were subject of our previous work [5–7]. Two negative-CTE (coefficient of thermal expansion) reinforcements are used as the third phase: 1) short carbon fiber and 2) zirconium tungstate.

Short carbon fiber composites

Short carbon fibers (SCFs) are a scrap material from the production of continuous fiber reinforcements. These fibers (approximately 7 μm diameter) can be milled to a variety of lengths for various applications. Not only are SCFs a cheap and widely available commodity, but CTE reduction with SCFs is well documented. PAN (polyacrylonitrile)-based SCFs have a slightly negative CTE (–0.5 ppm $°C^{-1}$) and high modulus (~250 GPa) in the longitudinal direction of the fiber, which makes CTE reduction efficient. For these reasons, short carbon fibers have long been used as a modifier for thermoplastics and there has been extensive use of short carbon fibers in epoxies [8–10]. For the reduction of composite CTE, short carbon fibers in an epoxy matrix reduced the CTE of the composite from 60 ppm $°C^{-1}$ to less than 10 ppm $°C^{-1}$ for loadings of up to 45 vol% [10]. However, there is a lack of literature on short carbon fibers with cyanate esters. This may be due to the fact that the low viscosity of cyanate esters prior to cure makes it impossible to create a useable composite without modifying the rheological behavior of the prepolymer.

Zirconium tungstate composites

Zirconium tungstate (ZrW_2O_8) is one of a small number of materials that exhibit isotropic negative thermal expansion and its behavior is unique because it has such a strongly negative CTE over a very wide temperature range (between –8.7 and –4.9 ppm $°C^{-1}$ from 20 to 950 K) [11–13]. This ceramic material has

* Author for correspondence: mkessler@iastate.edu

1388–6150/$20.00

Akadémiai Kiadó, Budapest, Hungary
Springer, Dordrecht, The Netherlands

shown potential for significant reduction of the CTE of composite materials with polymer matrices, both in micro-particulate [14, 15] and nano-particulate form [16]. Shi and coworkers investigated polyester and epoxy matrix ZrW_2O_8 composites for electronic applications and found that filler content of 30 vol% reduced the composite CTE by 40% for polyester and by 67% for epoxy [14]. Weyer *et al.* investigated the reinforcement of a commercial cyanate ester, CTD 403, with ZrW_2O_8, measuring the CTE's of different cross-sections of cylindrical composite samples in which the filler had settled significantly [15]. The CTE's of cross-sections with fractions from 0 to 52 vol% were reduced by up to 80% (CTE of 13.6 ppm $°C^{-1}$ at 100°C for 52 vol%). Cross *et al*. continued the work of Weyer on the reduction in CTE of the CTD 403 cyanate ester by treating the ZrW_2O_8 with an aminosilane [17]. Settling was reduced slightly, but similar reductions in CTE were observed, such that it was concluded that the silane treatment had little to no effect on composite CTE [17]. Sullivan and Lukehart investigated the CTE reduction of micro- and nano-particulate ZrW_2O_8/polyimide films [16]. Surface derivatization of the particles was shown to increase dispersion and loadings of up to 22 vol% reduced the film CTE by up to 30% [16]. Interestingly, the samples with the lowest loading (0.8 vol%) showed unusually large decreases in CTE (an average of 20%) [16]. Although the CTE for 0.8 vol% was well below what models would predict, the authors were not able to comment on the significance of their observation but confirmed their measurement with three independent batches of film [16].

Experimental

Three-phase composite samples were prepared at a volume fraction of 20% for both the SCF and ZrW_2O_8. Suspensions with and without fumed silica were used for settling comparison tests and catalyzed suspensions were cured at elevated temperatures and tested using dynamic mechanical analysis (DMA), thermomechanical analysis (TMA) and thermogravimetric analysis (TG).

Materials

The BECy monomer from Bryte Technologies (Morgan Hill, CA), EX-1510, was used as the matrix material. The supplied catalyst from Bryte Technologies was used in all cured samples at a loading of 3 phr (parts per hundred resin). Polyacrylonitrile (PAN)-based milled carbon fiber (Fortafil 341, CAS No.: 07440-44-0, density=1.74 g cm^{-3}) was supplied by Toho Carbon Fibers, Inc., Rockwood, TN (a subsidiary of Toho Tenax Co., Ltd.). This product is a loose, black, powdery material comprised of unsized 7 μm diameter fibers with lengths ranging from 75 to 150 μm. Zirconium tungstate was supplied by ATI Wah Chang, Albany, Oregon (CAS No.: 16853-74-0). This white powder has a density of 5.07 g cm^{-3}. Hydrophilic fumed silica was supplied by Degussa (Frankfurt, Germany) under the trade name of AEROSIL® 200 (CAS No.: 112945-52-5, synthetic amorphous, pyrogenic silica, purity ≥99.8%, density=2.2 g cm^{-3}). AEROSIL® 200 has an average primary particle diameter of 12 nm and a specific surface area of 200 m^2 g^{-1} [18].

Specimen manufacturing

For SCF composites, BECy monomer/fumed silica suspensions of 5 phr were prepared using the procedure outlined in our previous work [7] except sonication of the suspensions was eliminated. After catalyst addition, the fiber was added while mixing with a high shear blade (25 mm diameter) at 2000 rpm for 10 min. Carbon fiber was then added in a stepwise fashion until the desired composition, 20 vol%, was reached (based on the total volume with fumed silica and a SCF density of 1.74 g cm^{-3}). Additionally, suspensions without catalyst were prepared in the same manner for use in settling tests.

Initial prepolymer samples made using the as-received milled carbon fiber product were very 'clumpy'. This was attributed to agglomeration of fibers into small 'balls', which occurs during manufacturing and storage. The described mixing strategies were not sufficient to break up these clumps of fibers. In order to solve this problem, the as-received product was forced through a No. 100 (150 μm) Cole-Parmer USA Standard Test Sieve prior to addition to the prepolymer. This change nearly eliminated the inhomogeneity in the prepolymer and polymer samples.

For ZrW_2O_8 composites, BECy monomer was preheated to 60°C and the ZrW_2O_8 powder (dried prior to addition at 120°C for 2 h) was added in a stepwise manner to a loading of 112 phr (corresponding to 20 vol%). The partially dispersed mixture was processed using a Sonic Dismembrator (Model 100, Fisher Scientific, Hanover Park, IL) with 3.2 mm diameter probe tip for 30 sec at a frequency of 23 kHz. The power output ranged between 16 and 18 Watts during sonication. After sonication, the suspension was again mixed for 2 min at 2000 rpm. The fumed silica (dried prior to addition at 120°C for 2 h) was added to a level of 5 phr during mixing. The temperature of the suspension was maintained between 50 and 65°C throughout the entire process. Before silica addition and prior to catalyst addition, two portions of the dispersed suspensions (BECy/ZrW_2O_8 and BECy/ZrW_2O_8/silica) were set aside for settling tests. For the remaining material,

catalyst was added to the suspension at a level of 3 phr and mixed at 2000 rpm for 2 min.

For preparation of cured composite samples, catalyzed suspensions of both types (SCF and ZrW_2O_8) were transferred into high-temperature silicone rubber molds (27 mm×48 mm×8 mm) and degassed at 60°C for 1 h under vacuum at 23.4 mm Hg and then placed in a convection oven (preheated to 60°C) for the final curing process (heat to 180°C at 1°C min^{-1}, hold for 2 h, heat to 250°C at 1°C min^{-1}, hold for 2 h and cool to ambient at 5°C min^{-1}). Samples were machined from the solid block of material using a diamond blade saw (TechCut 5™ Precision Sectioning Machine with Diamond Wafering Blade, Low-Concentration Diamond Metal Bonded, 6"×.020"×1/2", Allied High Tech Products, Inc.). Specimens for thermomechanical analysis (TMA) were machined to 3 mm×3 mm×6 mm. Specimens for dynamic mechanical analysis (DMA) were machined to 23 mm×6 mm×1.6 mm, such that the thickness of each specimen varied by less than 15 μm over its length.

Methods

Samples for DMA were tested using a TA Instruments (New Castle, Delaware, USA) DMA (Dynamic Mechanical Analyzer) Q800 with LN_2 GCA (Gas Cooling Accessory) from 30 to 330°C at a heating rate of 3°C min^{-1}. A constant amplitude of 20 μm at 1 Hz was applied throughout the test, with a static load tracking at 150% of the dynamic force. A low-friction three-point bending fixture with a length of 20 mm was utilized for each test.

Thermomechanical testing was completed using a TA Instruments (New Castle, Delaware, USA) TMA (Thermomechanical Analyzer) Q400. Samples were under a static force of 50 mN through two heating and cooling cycles from 30 to 300°C at a heating rate of 5°C min^{-1} under helium purge at 50 mL min^{-1}. For SCF composites, the TMA samples were tested in the longest dimension, but for ZrW_2O_8 composites, the samples were tested perpendicular to the settling direction. Thermogravimetric analysis was performed using a TA Instruments (New Castle, Delaware, USA) TG (Thermogravimetric Analyzer) Q50. Portions of the TMA samples were heated in the TG from room temperature to 1000°C at 20°C min^{-1} under air purge at 60 mL min^{-1}.

Results and discussion

Settling

Our previous work on fumed silica/cyanate ester nanocomposites has shown that the addition of fumed silica to the BECy monomer imparts thixotropic behavior. Rheological testing showed that the viscosity of BECy/fumed silica suspensions is high at low shear rates and low at high shear rates [7]. For 5 phr fumed silica, the viscosity at room temperature is 3.6 Pas at 0.1 s^{-1} and 0.32 Pas at 100 s^{-1}, while the BECy monomer has a visocity (without catalyst) of 0.068 Pas [7]. Additionally, the viscosity of the suspensions builds over time, such that after one hour at rest, the viscosity will rise to over 47 Pas [7]. For three-phase composite adhesives, fumed silica allows for fillers with high densities to be incorporated into the low viscosity BECy monomer without phase separation during storage. Figure 1 shows composite suspensions prepared with and without fumed silica, showing the pronounced settling without fumed silica and the lack of settling with fumed silica.

During thermal curing at elevated temperatures (with added catalyst), the cyanate ester prepolymer will experience a drop in viscosity before gelation occurs (the viscosity of the BECy monomer reduces to $5.6 \cdot 10^{-3}$ Pas at 60°C). For the SCF three-phase composite, this drop was not enough to induce phase separation during cure, but for the ZrW_2O_8 composite, an obvious layer of settled ZrW_2O_8 was observed at bottom of the molded part. Figure 2 shows a picture of a ZrW_2O_8 composite sample with settled layer. The sample was sectioned at the interface between the layers and the samples were used for TMA and TG evaluation.

After TMA evaluation, the samples were heated to 1000°C in the TG (under air purge) to remove all cured BECy. TG data for the cured BECy, BECy/fumed silica composite (BECy-FS) and each ZrW_2O_8 composite sample (top: BECy-FS/Z10 and bottom: BECy-FS/Z58) are shown in Fig. 3. In Table 1, the temperature at which the maximum rate of decomposition occurs ($T_{dm/dT,max}$) and the final mass are recorded. All samples showed a similar decomposition profile, with a maximum rate of decomposition between 435 and 447°C. While

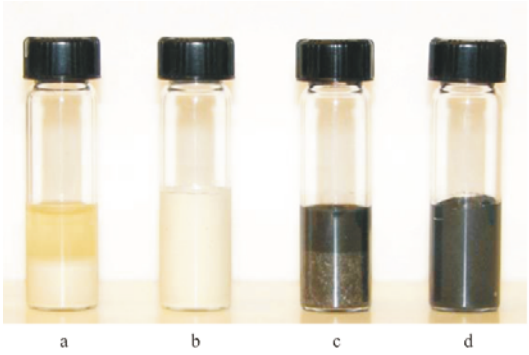

Fig. 1 20 vol% samples after settling at room temperature for 90 h and 60°C for 6 h, a – BECy/ZrW_2O_8, b – BECy/ZrW_2O_8/fumed silica, c – BECy/SCF, d – BECy/SCF/fumed silica

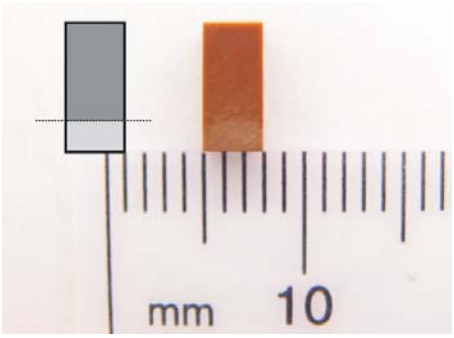

Fig. 2 Three-phase ZrW_2O_8 composite sample, showing settling of ZrW_2O_8. Sample was cut at line indicated for TMA and TG evaluation

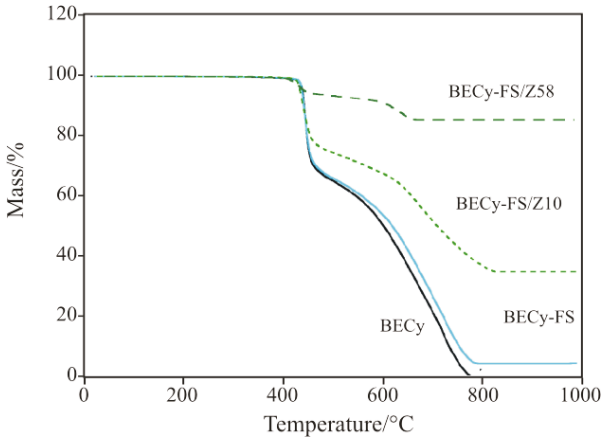

Fig. 3 TG data for cured BECy sample with fumed silica (BECy-FS) and ZrW_2O_8

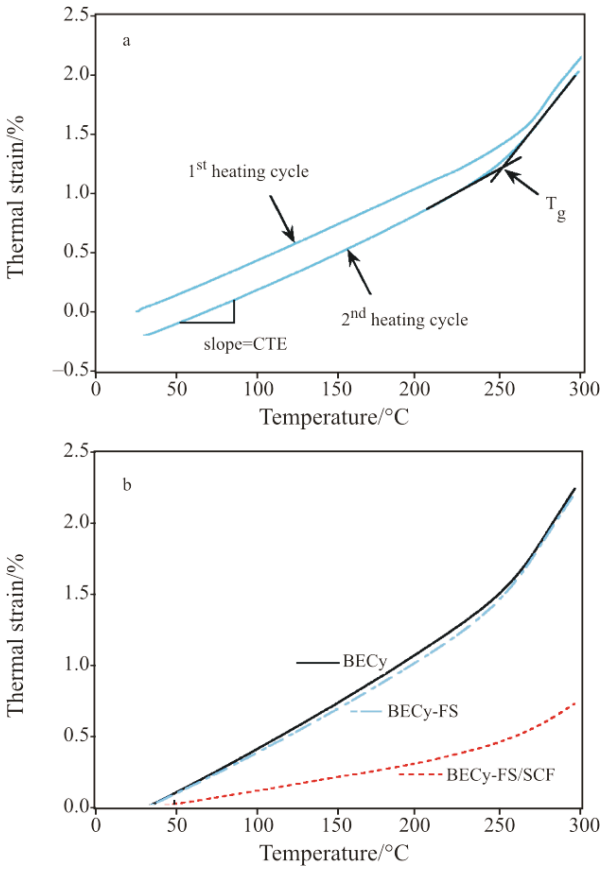

Fig. 4 Thermal strain *vs*. temperature for a – BECy-FS (1st and 2nd heat) and b – BECy, BECy-FS and BECy-FS/SCF samples, 2nd heating cycle, with thermal strain normalized to zero at 30°C

Table 1 TG data for BECy, BECy-FS, top (Z10) and bottom (Z58) ZrW_2O_8 samples

Sample name	$T_{dm/dT,max}$/°C	Final mass/ mass%	ZrW_2O_8/ vol%
BECy	446.6	0.0	–
BECy-FS	445.0	4.5	–
BECy-FS/Z10	443.0	33.5	10.2%
BECy-FS/Z58	435.1	85.6	57.7%

the addition of fumed silica did not change the decomposition significantly, the ZrW_2O_8 reduced this temperature by almost 12°C for the highest loading (BECy-FS/Z58). From the remaining mass fraction, the actual volume fraction of the sample tested in the TMA was determined, using the appropriate densities and assuming a constant 5 phr fumed silica throughout the entire sample.

Thermal expansion

From TMA evaluation, thermal strain *vs*. temperature curves for the 1st and 2nd heating cycles of BECy-FS are shown in Fig. 4a. The data from the 1st heating phase provides information on the thermal and mechanical history of the specimen, but after annealing above T_g, the 2nd heating phase provides the true material behavior only [19]. For this reason, the true CTE of the material is taken from the 2nd heating cycle and is equal to the slope of the curve shown. The T_g is observed as a large rate of increase in thermal strain (step increase in CTE) and is marked as the onset in this increase in Fig. 4a. The second heating cycle curves are shown for BECy, BECy-FS and BECy-FS/SCF in Fig. 4b.

The 1st heating cycle thermal strain *vs*. temperature data for the ZrW_2O_8 composites showed an interesting feature. There is a large increase in strain and CTE around 115 to 120°C. Figures 5 and 6 show the thermal strain and CTE data *vs*. temperature for the two ZrW_2O_8 composites.

The increase in strain around 115 to 120°C may be attributed to a transition in the ZrW_2O_8 from γ-ZrW_2O (an orthorhombic symmetric phase) to α-ZrW_2O (an acentric cubic phase). With sufficient pressure (200 MPa at ambient temperature), ZrW_2O_8 will transition to the undesirable γ-phase from either α or β (a centric cubic

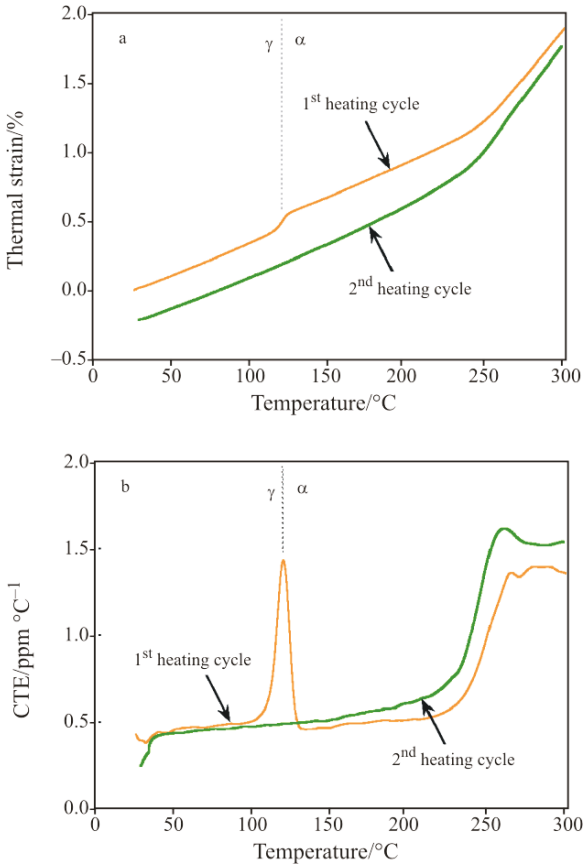

Fig. 5 TMA data for BECy-FS/Z10 sample, a – thermal strain *vs*. temperature, b – CTE *vs*. temperature

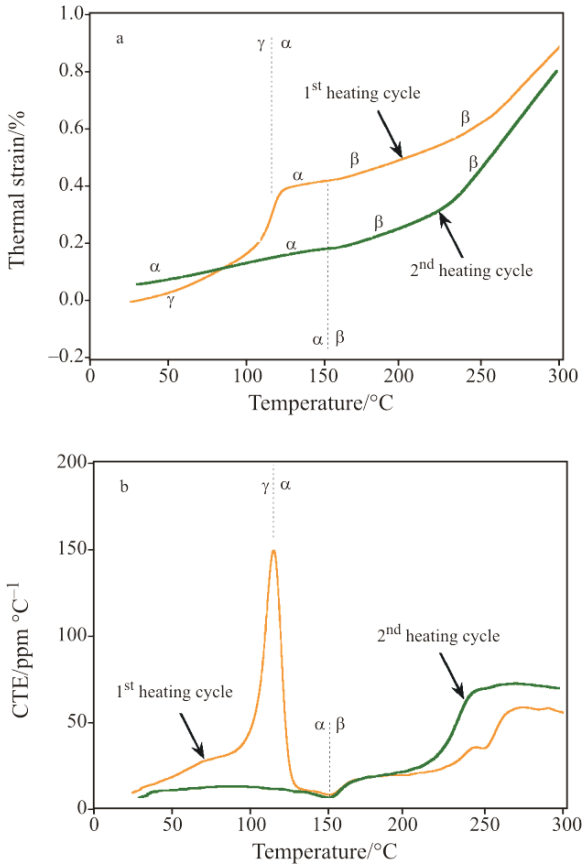

Fig. 6 TMA data for BECy-FS/Z58 sample, a – thermal strain *vs*. temperature, b – CTE *vs*. temperature

phase). The γ-phase is undesirable because its CTE is not as negative as the α-phase (only –1.0 instead of –8.7 ppm °C^{-1}). The pressure needed to produce this phase transition may be provided by the formation of residual stresses in the composite after gelation (which occurs at an elevated temperature) and during cooling from the final cure temperature (250°C) to room temperature. There is an extreme CTE mismatch between the matrix and filler, which would cause the matrix to contract heavily during cooling while the ZrW_2O_8 (with negative-CTE) actually expands during cooling. This may provide a sufficient compressive stress to induce the formation of the γ-phase.

Upon heating ZrW_2O_8 to between 117 and 137°C, the material is changed back to α. This transition is accompanied by a 5% increase in volume [12], thus explaining the increase in thermal strain and peak in CTE observed in Figs 5 and 6 near this temperature. After annealing the sample above the glass transition of the matrix, residual stresses are relieved; thus, the γ to α transition is not observed in the 2nd heating cycle.

In addition to the transition near 120°C, there is an additional transition evident in the high volume fraction ZrW_2O_8 sample (Z58) at about 150°C (Fig. 6). This may be attributed to a transition in the ZrW_2O_8 from α to β. This transition occurs between 150 and 177°C and changes the ZrW_2O_8 CTE from –8.7 to –4.9 ppm °C^{-1} [11]. The CTE *vs*. temperature data also has a minimum at 150°C, where the phase transition occurs. A brief summary of the properties and transitions of ZrW_2O_8 are shown in Table 2.

Table 2 Properties and transitions of ZrW_2O_8 [11–13]

Phase	CTE/ppm °C^{-1}	Density/g cm^{-3}
α-ZrW_2O_8	–8.7	5.08
β-ZrW_2O_8	–4.9	5.98
γ-ZrW_2O_8	–1.0	5.36

Transition	Temperature/°C	Pressure/MPa
α to β	150–177	0.101
α/β to γ	150–177	200.0
γ to α	117–137	0.101

A summary of the properties of the three-phase composites observed through TMA are shown in Table 3. For each composition, the T_g (from onset in 2nd heating cycle) and CTE values (at 50, 100, 150 and 200°C) are shown.

The CTE values for all compositions (2nd heating cycle) are plotted *vs*. temperature in Fig. 7. As expected, the CTE for all samples increases with temp-

Table 3 Thermal expansion values for three-phase composites, as well as onset T_g' from TMA (from 2nd heating cycle)

Composition			ZrW_2O_8 Phase	CTE/ppm °C^{-1}				Onset T_g/°C
Sample name	fumed silica	negative-CTE filler		50°C	100°C	150°C	200°C	
BECy	–	–	–	58.1	63.5	68.2	74.6	251.9
BECy-FS	5 phr (2.6 vol%)	–	–	55.8	60.0	65.1	71.8	245.8
BECy-FS/SCF	5 phr (2.1 vol%)	20.0 vol% SCF	–	17.2	19.1	19.2	23.0	251.8
BECy-FS/Z10	5 phr	10.2 vol% ZrW_2O_8	α	43.3	47.4	–	–	237.1
BECy-FS/Z10	5 phr	10.2 vol% ZrW_2O_8	β	–	–	–	61.2	237.1
BECy-FS/Z58	5 phr	57.7 vol% ZrW_2O_8	α	10.0	12.1	–	–	227.7
BECy-FS/Z58	5 phr	57.7 vol% ZrW_2O_8	β	–	–	–	21.4	227.7

erature. In Fig. 7a, the large increase in CTE near the end of the range is due to the glass transition of the composites. While the T_g of SCF composite is nearly identical to that of the neat BECy, it can be seen from Table 3 and Fig. 7 that increasing ZrW_2O_8 content reduces T_g substantially. This may be due to a reduction in crosslink density that occurs due to inclusion of the ZrW_2O_8 and exposure of the ZrW_2O_8 surface to the BECy during polymerization.

The addition of 20 vol% SCF and 5 phr fumed silica reduces the CTE of the BECy from 58.1 to 17.2 ppm °C^{-1} at 50°C and from 63.5 to 19. ppm °C^{-1} at 100°C. This represents a decrease compared to the neat BECy of 70.4 and 69.9% at 50 and 100°C, respectively. For ZrW_2O_8 in the α-phase, decreases in CTE compared to BECy of 83.8% at 50°C (10.0 ppm °C^{-1}) and 80.9% at 100°C (12.1 ppm °C^{-1}) are observed for 57.7 vol%. For the β-phase, a decrease of 71.4% is observed at 200°C (CTE from 74.6 to 21.4 ppm °C^{-1} for 57.7 vol%). The lower level of CTE decrease in this temperature range is due to the fact that the β-phase has a less negative CTE than the α-phase of ZrW_2O_8. Interestingly, during the α to β-transition, the CTE of the BECy-FS/Z58 reduces to a minimum of 5.3 ppm °C^{-1} at 150.8°C (91.9% decrease from neat BECy). This extreme decrease is CTE is only observed over a small temperature range and may be due to the decrease in volume (increase in density) of the ZrW_2O_8 during the transition.

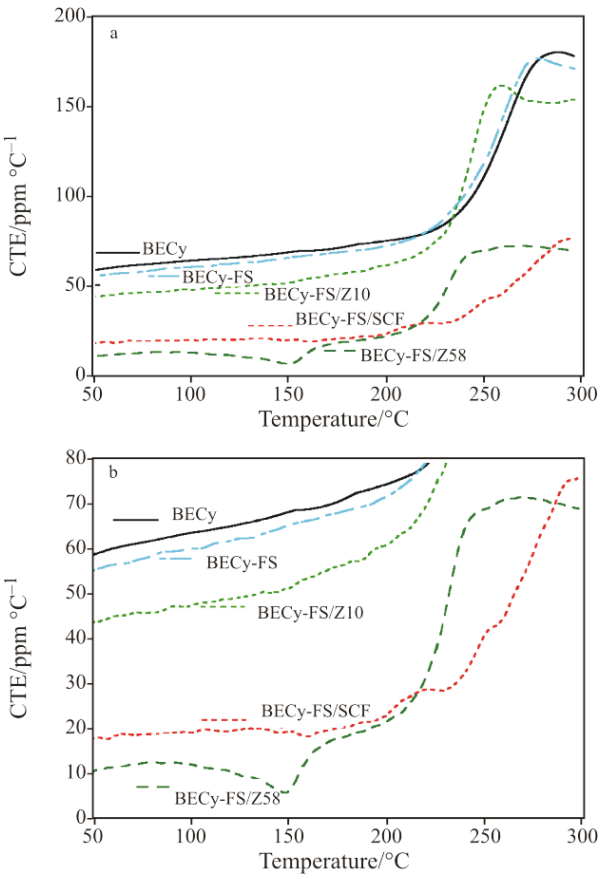

Fig. 7 CTE *vs.* temperature comparison for all samples, a – all data, b – close-up

Dynamic mechanical analysis

The storage moduli and tanδ values are plotted *vs.* temperature for the four different systems in Fig. 8. The ZrW_2O_8 sample was cut from the original partially settled block such that the composition varied across the width of the beam (the average loading across the specimen is 20 vol% ZrW_2O_8). The sample was heated from 30 to 330°C at 3°C min^{-1} two times to condition the sample (data not shown) by transitioning the embedded ZrW_2O_8 from the γ to the α–phase and relaxing the residual stresses that developed in the polymer matrix during cure (and contributed to the initial pressure induced γ-phase transition).

As can be seen from Fig. 8, the storage moduli in both the glassy and rubbery region increase from neat BECy, to BECy with 5 phr fumed silica (BECy-FS), to BECy with fumed silica and ZrW_2O_8 (BECy-FS/Z20), to BECy with fumed silica and 20 vol% short carbon fiber (BECy-FS/SCF). Similarly, the tanδ peak magnitudes decreased from BECy to BECy-FS to BECy-FS/SCF to BECy-FS/Z20. There is also a substantial decrease in glass transition temperature (as measured by both

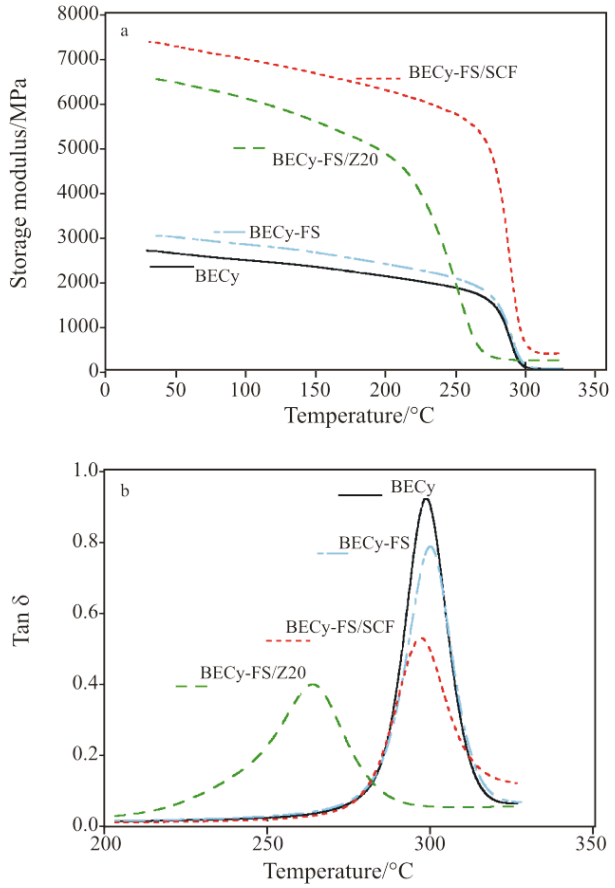

Fig. 8 Storage modulus *vs*. temperature, a – and tanδ *vs*. temperature, b – comparisons for all samples

onset of the drop in storage modulus or by the tanδ peak) for the ZrW_2O_8 composite, confirming the concomitant results in the TMA measurements.

Conclusions

Three-phase composites based on fumed silica/cyanate ester nanocomposites and negative-CTE fillers were demonstrated for feasibility. Without fumed silica, complete phase separation was observed, but with fumed silica, more useable composites were manufactured. Settling was virtually reduced for the SCF samples, but settling was not completely eliminated for the ZrW_2O_8 composites. The SCF composites exhibited significant enhancements in modulus and significant reduction in CTE. ZrW_2O_8 composites showed interesting thermal expansion behavior, which was attributed to phase transitions in the ZrW_2O_8. The lowest CTE's observed were for the highly loaded ZrW_2O_8 composite and the SCF composite. The addition of ZrW_2O_8 reduced the T_g of the composite significantly, but T_g's for other composites were similar to that of the neat resin.

Acknowlegements

This material is based upon work supported under a National Science Foundation Graduate Research Fellowship. Additional support from the Strategic Environmental Research and Development Program (SERDP), under the 'Environmentally Benign Repair of Composites Using High Temperature Cyanate Ester Nanocomposites' project (Project Number WP-1580) is gratefully acknowledged. Special thanks are extended to Mr. Ben Mac Murray for his help in the preparation of samples and to Mr. Xia Sheng, Mr. Louis Charles and Dr. Mufit Akinc for their technical support and thoughtful discussion. The authors would also like to thank Degussa, Toho Tenax Co. and ATI Wah Chang for providing samples of fumed silica, SCF and ZrW_2O_8.

References

1 D. A. Shimp and W. M. Craig, Jr., Proc. of the 34th Annual Int. SAMPE Symp., 1989, pp. 1336-1346.
2 W. K. Goertzen and M. R. Kessler, Compos. Part A-Appl. S., 38 (2007) 779.
3 J. Wen and D. Bryant, Adhes. Seal. Ind., 6 (1999) 48.
4 CAB-O-SIL® M-5 Product Technical Data. Billerica, MA: Cabot Corp., 2000.
5 W. K. Goertzen and M. R. Kessler, Compos. Part A-Appl. S., in press.
6 W. K. Goertzen and M. R. Kessler, J. Appl. Polym.Sci., in press.
7 W. K. Goertzen and M. R. Kessler, Polym. Eng. Sci., in press.
8 C. Kaynak, O. Orgun and T. Tincer, Polym. Test., 24 (2005) 455.
9 X. Gong, Polym. Adv. Technol., 7 (1996) 141.
10 M. Y. Jeong and D.G. Lee, J. Mater. Process. Technol., 63 (1997) 375.
11 A. W. Sleight, Annu. Rev. Mater. Sci., 28 (1998) 29.
12 J. S. O. Evans, J. D. Jorgensen, S. Short, W. I. David, R. M. Ibberson and A. W. Sleight, Phys. Rev. B, 60 (1999) 14643.
13 F. R. Drymiotis, H. Ledbetter, J. B. Betts, T. Kimura, J. C. Lashley, A. Migliori, A. P. Ramirez, G. R. Kowach and J. Van Duijn, Phys. Rev. Lett., 93 (2004) 025502-1.
14 J. D. Shi, Z. J. Pu, K.-H. Wu and G. Larkins, Proc. Mat. Res. Soc. Symp., 1997, pp. 229–234.
15 W. C. Weyer, W. M. Cross, B. Henderson, J. J. Kellar, L. Kjerengtroen, J. Welsh and J. Starkovich, Proc. 46th AIAA/ASME/ASCE/AHS/ASC Conf., 2005, pp. 3577–3593.
16 L. M. Sullivan and C. M. Lukehart, Chem. Mater., 17 (2005) 2136.
17 W. M. Cross, B. D. Henderson, W. C. Weyer, C. Kroetch, L. Kjerengtroen, J. Welsh and J. J. Kellar, Proc. SME – Func. Fill. and Nanoscale Min., 2006, pp. 127–140.
18 AEROSIL® Product Technical Information, Germany, Degussa, Frankfurt 2006.
19 G. W. Ehrenstien, G. Riedel and P. Trawiel, Therm. Anal. of Plast.: Theory and Pract., Carl Hanser Verlag, Munich 2004.

DOI: 10.1007/s10973-007-8804-2